Table 2. LOHs in PTCs with or without metastasis.

Chromosome	+ Metastasis	- Metastasis	P Value
1p36	7/12	5/14	
3p24	2/12	4/14	
3p12	0/12	3/114	
7p31	0/12	2/14	
9p21	6/12	8/14	
10q23	6/12	3/14	0.017
17p13	3/12	1/14	0.003
17q21	4/12	1/14	< 0.001
18q21	1/12	3/14	
21q22	3/12	3/14	
22q13	6/12	3/14	0.017

Yates' correction test.

Conclusions: 1. LOH at 1p34-36, 17p13 and 22q13 is significantly more common in BDC with metastasis compared to BDC without metastasis.
2. LOH at 10q23, 17p13, 17q21, and 22q13 is significantly more common in PTC with metastasis compared to PTC without metastasis.
3. LOH at 17p13 and 22q13 is shared by both BDC and PTC with metastasis, whereas LOH at 1p34-36 in BDC and LOHs at 10q23 and 17q21 is not shared.
4. Therefore, our results suggest that BDC and PTC share the same metastatic mechanisms that involve LOH at 17p13 and 22q13. The LOH signature may be clinically useful to better predict which carcinomas (breast and thyroid) might metastasize. More detailed studies to identified genes in these shared regions of LOH may provide insight into molecular mechanism of metastasis in these two tumor types.

Pediatrics

1863 Epithelioid Rhabdomyosarcomas: A Clinicopathologic and Molecular Study

R Alaggio, A Zin, A Rosolen, P Dall'Igna, G Bisogno, R Bertorelle. University of Padova, Padua, Italy; University Hospital Padova, Padua, Italy; Padua Hospital, University of Padua, Padua, Italy.

Background: Rhabdomyosarcoma (RMS), the most common pediatric soft tissue sarcoma is currently classified in 2 principal subtypes: embryonal (ERMS) characterized by variable genetic alterations including *TP53*, *RB1* and *RAS* mutations; alveolar RMS (ARMS), harbouring a gene fusion between *PAX3* or *PAX7* and *FOXO1*, with an aggressive clinical behaviour. Epithelioid RMS is a morphologic variant of RMS recently described in adults.

Design: 150 ARMS enrolled in Italian therapeutic protocols were reviewed in order to identify tumors with features of Epithelioid RMS and investigate their molecular features. Immunostainings (muscle specific actin, Desmin, Myogenin, AP-2β, EMA, cytokeratins, INI-1), reverse-transcriptase polymerase chain reaction (RT-PCR) assays to detect *MyoD1*, *myogenin*, and *PAX3/7-FOXO1* transcripts were performed. DNA sequencing of *TP53* was performed by capillary automated sequencer; *RB1* allelic imbalance (gain or loss) and homozygous deletion were analyzed by quantitative real-time PCR.

Results: Five Epithelioid RMS were identified. Clinical features are summarized in the table 1. Histology showed sheets of large cells without rhabdomyoblastic differentiation or anaplasia in 3 and prominent rhabdoid cells in 2; Necrosis in 4, often with a geographic pattern. Immunostainings showed: positive staining for INI, Desmin and Myogenin (scattered cells in 4, 70% in 1); EMA and MNF116 were positive in 2, AP-2β constantly negative. All tumors lacked *PAX/FOXO1* transcripts. *RB1* and *TP53* were wild type in 4 and 3 cases respectively, with mutation at R273H codon in 1.

Table 1

Case	Age/sex	Size	Site	Lymph-node Metastasis	Follow-up
1	9y/M	u*	HN-PM**	N1	ANED (8yr)
2	6y/M	3.3	HN-PM	N0	ANED (10yr)
3	13y/F	4	arm	N0	ANED (8yr)
4	11y/F	u**	arm	N0	u
5	8y/M	8.3	orbit	N0	ANED (4yr)

*unknown, **HN-PM head/neck parameningeal

Conclusions: RMS with epithelioid morphology rarely occurs in children. Lack of ARMS translocations, weak staining for myogenin and negative AP-2β suggest a potential relationship with ERMS, inline with by *TP53* mutation found in one case and by the favourable clinical course in the 3 patients with available follow-up.

1864 Pediatric Anaplastic Ependymoma: Morphoproteomics and Biomedical Analytics Identify Hypoxia Pathway Signaling and Provide Targeted Therapeutic Options

AQ Al-Ibraheemi, MF McGuire, RE Brown. UT Health-Medical School, Houston, TX.

Background: Relapsed, anaplastic ependymoma carries a poor prognosis, eventuating in death in approximately 90% of patients. Such tumors are largely chemoradioresistant. New therapeutic strategies will require defining the biology of anaplastic ependymoma. *Objective:* To profile pediatric anaplastic ependymomas using morphoproteomic techniques in an effort to identify pathogenetic commonalities amenable to therapeutic intervention and to employ biomedical analytics to translate such findings into targeted therapies. *Study Population: S*ix (6) pediatric patients (ages 3 to 10 years)with recurrent/progressive anaplastic ependymoma were included in this IRB approved study using morphoproteomic analysis.

Design: Morphoproteomics and biomedical analytics. Representative sections from formalin-fixed, paraffin-embedded sections of histopathologically proven cases of anaplastic ependymoma were received for morphoproteomic analysis.

Results: Hypoxia-inducible factor (HIF)-1 alpha expression with nuclear translocation was identified in four out of six tumors and showed correlative expression of:phosphorylated (p)insulin-like growth factor receptor; p-mammalian target of rapamycin (mTOR)[Ser2448] with nuclear translocation (favoring mTORC2); cyclo-oxygenase (COX)-2; p-p38 mitogen-activated protein kinase (MAPK)[Thr180/Tyr182]; secreted protein acidic and rich in cysteine (SPARC);and hypoxia/stemness markers to include CD133 and nestin.These coincided with the presence of ischemic-type coagulative necrosis in the same four cases. Biomedical analytics were then applied to the morphoproteomic analysis data. For each case, a scored profile was computed and used to generate the most likely biological pathway network model. The models revealed interactions with therapeutic agents that modulate hypoxia pathways including metformin, a histone deacetylase inhibitor (valporic acid), melatonin, celecoxib and doxorubicin

Conclusions: The application of morphoproteomics to recurrent/progressive anaplastic ependymoma cases reveals protein correlates of hypoxia pathway signaling which also accord with coagulative type necrosis in 4 out of 6 cases. This represents an adaptive pathway in such tumors to allow the emergence of chemoradioresistant populations and recurrent disease. Morphoproteomic analysis and biomedical analytics provide therapeutic options designed to target this adaptive pathway in cases in which the hypoxia pathway is identified.

1865 Correlation of Prenatal Diagnosis and Pathology Findings Following Dilation and Evacuation for Fetal Anomalies

CA Boecking, EA Drey, WE Finkbeiner. UCSF, San Francisco, CA.

Background: While pathology examinations are generally recognized as the "gold standard" for confirming clinical diagnoses, D&E procedures typically provide fragmented and/or incomplete specimens making clinical-pathological correlations difficult, imperfect or impossible. However, careful examination of fragmented fetal specimens is valuable and may confirm, supplement or correct diagnoses. In this study, we correlated pathology findings with prenatal diagnoses in D&E specimens.

Design: Clinical and pathology findings in 200 D&E specimens were correlated. Termination of pregnancy was based on abnormal karyotype in 90 cases and abnormal ultrasound examination in 110 cases. The pathology findings, sometimes multiple per individual case, were categorized into 1 of 4 groups (musculoskeletal, cardiac, genitourinary, or central nervous system [CNS]). Cases with multiple defects were also assigned to an additional category, Multiple Anomalies (MA).

Results: Ninety chromosomal abnormalities included trisomy 21 (48), trisomy 18 (23), trisomy 13 (8), and others (11). 51 (57%) of these cases showed at least one abnormality on pathology examination. In 110 cases where ultrasound led to D&E, at least one anomaly was confirmed in 76 (69%) specimens. In 22 of 54 cases of musculoskeletal anomalies, pathology examination confirmed the diagnosis. There were 15 cases with presumed cardiac defects; however, intact hearts were present in only 10 specimens. In these, examinations confirmed ultrasound findings in 6 and altered them in 4. Genitourinary anomalies were confirmed in 22 of 23 cases, with complete agreement in 14. Evaluating for CNS pathology proved challenging due to disruption from the D&E procedure. However, in 34 cases with ultrasound findings—anencephaly (22), encephalocele (4) and spina bifida (8)—the clinical diagnosis was confirmed in 53%. Since fetal anomalies are often complex and involve numerous organs, we also determined how often examinations could identify multiple abnormalities in a single case. Thus, in 68 MA specimens, abnormalities were identified in 48 with complete correlation in 8, partial correlation in 32, and 8 in which defects were incorrectly identified on ultrasound. Taking all categories into account, pathology studies yielded additional diagnostic findings in 21% of cases.

Conclusions: In a substantial number of cases, examination of fragmented fetuses corrects or refines prenatal diagnoses aiding subsequent genetic counseling.

1866 Recurrent *NCOA2* Gene Rearrangements in Congenital/Infantile Spindle Cell Rhabdomyosarcoma

JM Mosquera, A Sboner, L Zhang, N Kitabayashi, C-L Chen, YS Sung, M Edelman, MA Rubin, CR Antonescu. Weill Medical College of Cornell University, New York, NY; Memorial Sloan-Kettering Cancer Center, New York, NY; North Shore LIJ Health System, Flushing, NY.

Background: Spindle cell rhabdomyosarcoma (RMS) is a rare form of RMS with different clinical characteristics and behavior between children and adult patients. Its genetic hallmark remains unknown and it is debatable if there is a pathogenetic relationship between the spindle cell and the so-called sclerosing RMS.

Design: We studied two pediatric and one adult spindle cell RMS by next generation RNA sequencing. Data was analyzed using FusionSeq, a modular computational tool for gene fusion discovery. Additional 14 spindle cell RMS (from 8 children and 6 adults) and 4 sclerosing RMS (from 2 children and 2 adults) were screened by FISH.

Results: *SRF-NCOA2* gene fusion was detected in a spindle cell RMS from a posterior neck in a 7 month-old child. The fusion matched the tumor karyotype and was further confirmed by FISH and RT-PCR, which showed fusion of *SRF* exon 6 to *NCOA2* exon 12. *NCOA2* rearrangements were identified in 2 additional spindle cell RMS from a 3 month-old and a 4 week-old child, both arising in the chest wall. In the latter tumor, *TEAD1* was identified by rapid amplification of cDNA ends (RACE) to be the *NCOA2* gene fusion partner. All others were negative for *NCOA2* rearrangement.

Conclusions: Despite similar histomorphology in adults and young children, these results suggest that spindle cell RMS is a heterogeneous disease genetically as well as clinically. Our findings also support a relationship between *NCOA2*-rearranged spindle cell RMS occurring in young childhood and the so-called congenital RMS, which often displays rearrangements at 8q13 locus *(NCOA2)*.

1867 Infections in a Children's Hospital Autopsy Population

J Springer, R Craver. Louisiana State University Health Science Center, New Orleans, LA.

Background: Despite advances in antimicrobial therapy, infections/inflammatory lesions may frequently cause or contribute to death in children.

Design: We retrospectively reviewed all autopsies performed at a children's hospital from 1986-2009 and categorized infectious complications as 1)underlying cause of death,2) mechanism of death complicating another underlying cause of death,3) contributing to death 4) agonal or infections immediately before death 5) incidental. Infectious complications were then separated into 3-8 year groups to identify trends over the years.

Results: There were 1369 deaths over 24 years, 608 (44%) underwent autopsy at the hospital, another 122 (8.9%) were coroner's cases not performed at the hospital. There were 691 infectious conditions in 401 children (66%, 1.72 infections/infected patient).There were no differences in the percentage of autopsies with infections over the years, although the number of total infections decreased in the last 8 year period. The number of infections /patient varied over the different time groups. By categories, there were 85 (12.3%), 237(34.3%), 231 (33.4%), 82 (11.9%), and 56(8.1%) infections. The distribution remained similar over the time groups, with the exception of more category 2 and less category 3 infections in 2002-2009 compared to 1994-2001. Leading infectious diseases/complications include bronchopneumonia (188), sepsis (144),acute meningitis (35), pneumonitis (33- including 19 with specific viral agents identified),peritonitis (29), tracheobronchitis (24), necrotizing enterocolitis (19), gastritis (15) disseminated Candida (15), and lymphocytic myocarditis (14). Sepsis was significantly less frequent (p=.0041) in 2002-2009 compared with earlier periods. 159 agents of sepsis in 144 patients included 67 Gram positive cocci, 70 Gram negative rods, 7 other, 15 clinical. Enterococcus was the most common(22). Bacterial meningitis was significantly more frequent in the first time period (p=.0061) compared to the later periods. Strep. pneumoniae was the overall most frequent cause(10).

Conclusions: 66% of pediatric autopsies at a Children's Hospital had an inflammatory lesion, and was stable over the time studied. Most are the mechanism of death or a significant contributing factor, rather than the underlying cause of death. The decrease in meningitis after the 1986-1993 period may be partially attributed to the H. flu vaccine. The decline in deaths with sepsis may be due to increased awareness, education, and standardization of treatment in the institution for recognition and treatment of septic shock.

1868 A Morphometric Study To Establish Subjective Index of Cerebellar Hypoplasia: A Special Emphasis on Cerebellar Hypoplasia in Trisomy 18

Y Tanaka, M Tanaka, R Ijiri, K Kato, K Gomi, Y Itani, H Ishikawa, S Yamashita. Kanagawa Children's Medical Center, Yokohama, Kanagawa, Japan.

Background: Cerebellar hypoplasia (CH) is one of the common abnormalities reported in trisomy 18 (T18) and has been described also in several disorders other than T18. However, CH is a poorly defined condition and no critical morphometric standard for CH has been established.

Design: Nineteen cytogenetically confirmed T18 cases and 63 age-matched control patients were selected from the autopsy files of Kanagawa Children's Medical Center during the last 22 years. In order to evaluate "congenitally small cerebellum", we excluded patients whose ages were more than 6 days. After fixation in buffered formalin for more than two weeks, the cerebrum was cut-off at the level of mid-brain and the brain stem was cut-off at the level of inferior collicles under the standard protocol. The weights of the cerebrum, the brain stem, and the cerebellum were measured precisely. The entire brain weight (EBW) was defined as a sum of the weights of the three parts. Several weight ratios, including the cerebellum weight (CLW) to the EBW, the CLW to the body weight (BW), and the cerebrum weight (CRW) to the BW, were calculated.

Results: All 19 patients with T18 were delivered at over 30 weeks of gestation and were small for gestational age. The BW at autopsy ranged from 575g to 2,538g. The EBW after formalin-fixation ranged from 140.7g to 390.9g. The CLW ranged from 3.90g to 15.48g. The CLW/EBW of all T18 patients was below 4% ranging between 2.59% to 3.96%. Only 3 of the 63 age-matched controls showed the CLW/EBW to be below the standard range or within the range of T18 patients (Figure 1). Diagnoses of the 3 patients were thanatophoric dysplasia (2 patients) and Bowen-Conradi Hutterite syndrome (1 patient), both of which are considered to have CH.

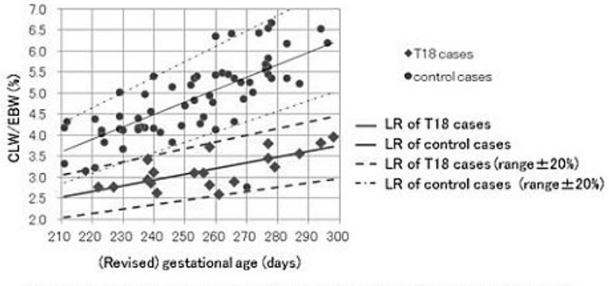

Figure 1 Graph showing standard ranges of CLW/EBW and values of CLW/EBW in T18 patients.
T18: trisomy 18 CLW: cerebellar weight EBW: entire brain weight LR: linear regression.

The CLW/BW was apparently lower in T18 cases than control patients, and the CRW/BW was slightly higher in T18 cases than in control patients.

Conclusions: Although standard for CH is difficult to define, the CLW/EBW obtained from the T18 patients seems to show a distinct tendency. The graph, shown in this abstract, is useful and may serve as a guideline to define CH, with linear regression +20% of T18 cases and/or linear regression -20% of control cases being the borderline for CH.

1869 Expression of Disialoganglioside GD2 in Neuroblastomas of Patients Treated with Immunotherapy

T Terzic, P Teira, S Cournoyer, M Peuchmaur, H Sartelet. Centre Hospitalier Universitaire Sainte-Justine, Montreal, QC, Canada; Hopital Universitaire Robert-Debre, Paris, France.

Background: Neuroblastoma, a malignant neoplasm of the sympathetic nervous system, is one of the most aggressive pediatric cancers with a tendency for widespread dissemination, relapse and a poor long term survival, despite intensive multimodal treatments. Recent use of immunotherapy (a chimeric human-murine monoclonal antibody ch14.18 directed against a tumor-associated antigen GD2, a disialoganglioside) to treat minimal residual disease has shown improvement in event-free and overall survival of high-risk neuroblastomas. However, some patients are resistant to immunotherapy. Therefore, the aim of the study was to analyze GD2 expression in neuroblastomas and see if the resistance to immunotherapy could be explained by the poor expression of GD2.

Design: We realized an immunohistochemical study on 140 cases of neuroblastomas included in TMAs and on 17 frozen specimens of neuroblastomas with an anti-GD2 antibody which has the same epitope as the one used in immunotherapy (monoclonal mouse antibody, 14G2A clone). The intensity of staining was graded as follows: "0", "1+", "2+", 3+" and "4+" when 0%, 1-25%, 26-50%, 51-75% and 76-100% of tumor cells respectively showed positive expression. The immunohistochemical results were interpreted without knowledge of the clinical characteristics. Among our patients, 12 have had immunotherapy and 3 of them showed resistance to it.

Results: Immunohistochemical expression of GD2 was found in 96.5% (135/140) of cases, among which 23 had between 1 and 25% of positive tumoral cells. There was a strong correlation between results in frozen and in paraffin sections. Immunostaining intensity was comparable in tumours and in metastasis (1.76 (mean intensity of GD2) vs 1.69) and also when patients were matched up for age (< or > than one year old, 1.82 vs 1.81) and MYCN amplification (2.00 vs 1.63). However, the mean intensity of GD2 expression was significantly higher (2.66 vs 1.33, p-value 0.02) in patients who responded versus those who were resistant to immunotherapy.

Conclusions: The observations of immunohistochemical expression of GD2 in our study show that most neuroblastomas express GD2, but most importantly that there is a significant difference in tumoral expression of GD2 between patients who respond and those who are resistant to immunotherapy. Thus, immunostaining with GD2 could become an important tool in deciding which patients should receive immunotherapy and so avoid overtreatment, but larger studies should be completed beforehand.

Pulmonary

1870 Combining Inhibitor of DNA – Binding Proteins and Angigenic Markers Expression Predict Long Term Survival of Patients with Non-Small Cell Lung Cancer

L Antonangelo, TS Tuma, FS Vargas, ER Parra, RM Terra, M Acencio, VL Capelozzi. University of Sao Paulo Medical School, São Paulo, Brazil.

Background: Inhibitor of DNA binding (Id) proteins is an emerging promise as biologic marker on oncogenic transformation, cancer progression and tumor angiogenesis, the last, by the regulation of vascular endothelial growth factor (VEGF) expression.

Design: We evaluated Ids (1, 2 and 3), VEGF expression and microvessel density (CD34+) in tumor and stromal cells and their impact on survival of 85 patients with surgically excised lung squamous cell carcinoma and adenocarcinoma. Immunohistochemistry and morphometry were used for the quantitation and Kaplan-Meyer survival curves and Cox regression for the statistical analyses.

Results: It was found that high Id-1 and VEGF expression and high microvessel density were associated with worse prognosis (Log Rank Test, $p<0.001$). The Cox model controlled for histological type, age, lymph node stage, Ids, VEGF and microvessel density demonstrated that age, lymph node stage, Id1 and Id3 expression and vascular density were significantly associated with overall survival. A point at the median for Id1, Id3 and vascular density divided patients into 2 groups of different prognosis. Those with higher expression of Id1, Id3 and vascular density had a higher risk of death than those with lower Id-1, Id-3 and microvessel density.

Conclusions: Inhibitor of DNA binding (Id) proteins and vascular density are strongly related to prognosis, suggesting that treatment strategies aimed for preventing high Ids synthesis, or local responses to angiogenesis may have impact on NSLC survival.

1871 Histologic Spectrum and Clinical Significance of Granulomatous Inflammation in Pulmonary Aspergillosis: A Study of 13 Cases with Comparison to Mycetomas and Invasive Aspergillosis

JF Back, S Mukhopadhyay. State University of New York Upstate Medical University, Syracuse, NY.

Background: The significance of granulomatous inflammation in pulmonary aspergillosis is not well understood. Prior studies have suggested that granulomatous inflammation is the histologic correlate of a tuberculosis-like progressive cavitary disease known as chronic necrotizing aspergillosis. The aim of this study was to describe the histologic spectrum of granulomatous inflammation in pulmonary aspergillosis and determine its clinical significance.

Design: Biopsied or resected cases of pulmonary aspergillosis over an 11-year period (1990-2011) were reviewed. Cases that showed granulomatous inflammation were compared with mycetomas and invasive aspergillosis. Clinical, radiologic and